1st IAA Conference on Space Situational Awareness (ICSSA)

Orlando, FL, USA

IAA-ICSSA-17-06-34

Orbital Probability of Collision using Orthogonal Polynomial Approximations

Austin B. Probe[1], **Christopher T. Shelton**[1], **Tarek A. Elgohary**[2], **John L. Junkins**[1]

[1] *Texas A&M University, College Station, TX 77843, (979) 845-7541, abprobe88@tamu.edu.*

[2] *University of Central Florida, Orlando, FL 32816, (407) 823-4379, elgohary@ucf.edu*

Keywords: *Uncertainty Quantification, Probability, Polynomial Approximation*

A new method for propagating uncertainty through a general nonlinear dynamical model with a parametric model of perturbations (such as aerodynamic drag) is developed. The model is constructed such that all of the model uncertainty is assumed to be embodied in a random vector of parameters. Initial state errors and the uncertain parameters are assumed to belong to specified (known) probability density functions (PDFs). In lieu of Monte Carlo Methods or other methods devised to characterize uncertainty, the present method identifies the region of extreme probability at the time of interest and populates that region with structured points and identifies the associated probability based on the a-priori PDF. By this method, these controllably dense points throughout the state space lead to an approximation for the non-linearly distorted non-Gaussian PDF at an arbitrary time t with a rigorous relationship to the a-priori probability density, and therefore doing any probabilistic analysis reduces to operations on simple interpolation functions. The non-conservative effects of drag are also accounted for computing the PDF at the time of interest. The method is then applied to compute the probability of collision for cases of resident space objects (RSOs) and compared against classical probability of collision techniques (state transition matrix (STM) based methods). The present approach has proven effective in quantifying uncertainty and computing the probability of collision without relying on the computationally expensive Monte Carlo methods or the low order low fidelity STM based methods.

1. Introduction

An accurate assessment of an RSO state uncertainty is vital to answering questions related to key SSA challenges, such as conjunction analysis, probability of collision or uncorrelated track association, [1–8]. The State Transition Matrix (STM)

[1] Austin B. Probe, Ph.D. Candidate, Aerospace Engineering Department.
[2] Graduate Researcher, Aerospace Engineering Department.
[3] Assistant Professor, Mechanical and Aerospace Engineering Department.
[4] Distinguished Professor, Aerospace Engineering Department.

based methods assume that the dynamics are linear and the posterior PDF remains Gaussian,[9–11]. The Fokker-Planck equation, known to capture the evolution of the initially Gaussian PDF in nonlinear dynamical systems, can be solved numerically to capture the evolution of the PDF,[12–15]. The current standard method for high fidelity propagation of uncertainty is using Monte Carlo (MC) based methods to generate histograms or kernel density estimates,[16–18]. MC based methods tend to be highly accurate, but suffer from the drawback of high computational cost. Other recent methods to quantify uncertainty include Gaussian Mixture Models (GMMs) and Polynomial Chaos Expansions (PCEs) with several contributions to apply those methods to the orbit problem, [17, 19–24].

All of the above mentioned methods are not capable of providing a general description of the posterior PDF, especially at higher levels of uncertainty, without extreme cost. In provious work the method of orthogonal uncertainty quantification was introduced,[25]. By placing structured points at the time of interest in the regions of extreme probability, the method approximates the non-Gaussian PDF at the time of interest by associating it with the known a-priori PDF at the initial time. A simple step-by-step schematic for a one-dimensional system is shown in Figure 1. The method quantifies uncertainty at the time of interest t_f, given a known distribution at some initial time t_0. The known distribution at t_0 and the unknown distribution at t_f are represented by the solid and dotted lines, respectively as shown in Figure 1((1)). By knowing the initial probability distribution the extreme bounds can be determined and propagated forward in time as depicted in Figure 1((2)). Next, the region of extreme probability is populated with nodes (cosine nodes in our example) at the time of interest as in Figure 1((3)). The evaluation nodes are then back propagated in time and compared to the a-priori probability distribution to get a value for the probability density at the final time, Figure 1((4)). The values obtained from the a-priori PDF are then used to generate an analytical approximation for the posterior PDF as depicted in Figure 1((5)).

The method was shown to be highly efficient for analysis in lower dimensions and capable of accurately describing the posterior PDF with very high precision. It showed orders of magnitude improvement in computational cost when compared to the classical Monte Carlo approach. Remarkably, this approach makes the low probability density region of the PDF be much more accurately defined (than is routinely feasible via Monte Carlo, due to slow convergence and the associated high computational cost).

In this work, building on the previously developed approach, the approximation of probability for various RSOs in higher dimensions with non-conservative effects (atmospheric drag) is addressed. This probability analysis is used to compute the probability of collision for RSOs in six degrees of freedom in the presence of uncertainty in the velocity states. Several numerical examples are introduced and compared against existing methods such as traditional Monte Carlo methods. Additionally, two enhancements, one based on sparse grid quadrature and one leveraging Monte Carlo analysis, are introduced to address curse-of-dimensionality issues that arise in higher dimensions.

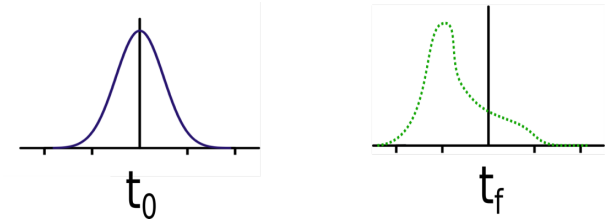

((1)) PDF at Initial and Posterior Times

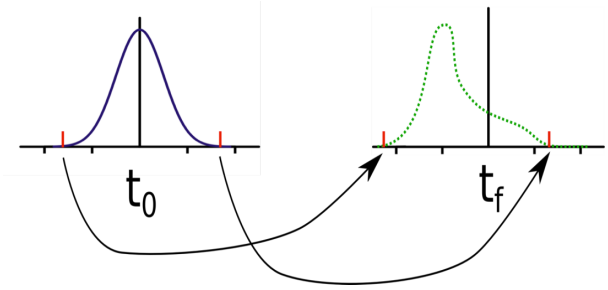

((2)) Propagation of the Extremal Probability Bounds

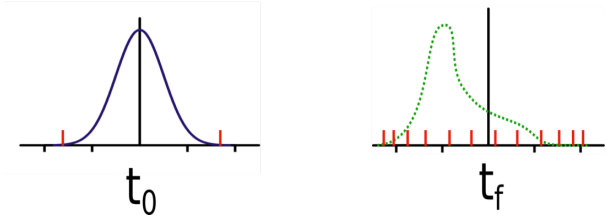

((3)) Nodes Distributed at Posterior Time

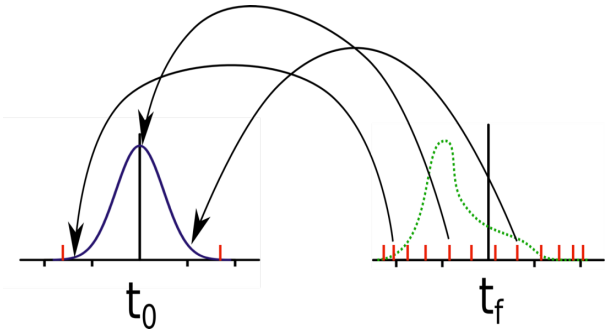

((4)) Back-propagation form the Evaluation Nodes to Determine the A-priori Probability Density

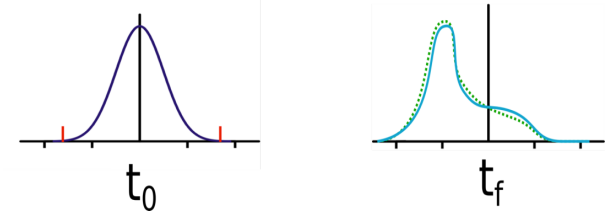

((5)) Probability Density Approximation Generated

Figure 1: Steps of Orthogonal Uncertainty Quantification

2. Extension of OPA for Orbital Dynamics

2.1. Region of Interest (ROI) Identification

It is possible to find the R two dimensional problem by sweeping along an extremal probability contour. However, if the method was then extended into 3 dimensions it would be analogous to finding the bounds on a constant probability surface. In the simplest case this would require the identification of evenly space points on a sphere. This challenge is known as Thomson problem, which originally dealt with finding the minimum energy configuration for electrons on a unit sphere. This problem is famously unsolved, and this does not even consider the difficulty when examining more than 3 dimensions, [26]. In light of this difficulty, a different method was devised that relies on a slightly modified version of Liouville Monte Carlo (LMC), [25]. Instead of spanning the entire probability space using LMC, points are only propagated along trajectories that originate from a surface where the value of probability density matches the extreme value of interest. These points are selected by first defining a specific probability and a value for a random state arbitrarily chosen from the range compatible with selected probability. Then each other state is defined in a random order, again randomly selecting a value compatible with the remaining probability, until the final state remains. This final state is defined by the other states and the state probability. The results of this constant probability LMC can then be used to find the bounds of the extremal region. This method requires the same order of forward propagations in two dimensions as method of uniformly sweeping around the contour of extremal probability and is easily extensible to higher dimensions. In order to find the region of intersection in higher dimension, constant probability LMC is used. Enough trajectories are propagated from uniformly distributed initial conditions with the defined extremal probability to define a region of the state space spanned by the reasonable terminal states of the objects being considered. An example result of this process can be seen in Figure 2. For cases where the intersection of probabilities is being considered, such as probability of collision, the combined ROI can be limited to the overlap of two individual ROIs; As demonstrated with a pair of 3D ROIs in Figure 3.

2.2. Dealing with Volume Change

The probability density is no longer conserved when considering non-conservative systems. However, since the total probability within the PDF must be constant, the volume of the probability must be conserved. Consequently, the probability density value is scaled proportionally to the change in the volume at each evaluation node. This change in volume can be computed by comparing the volume surrounding evaluation nodes at both the initial and final configurations. For any two dimensional case, the volume change can be estimated by constructing a series of triangles with the evaluation nodes as their vertices. The a-priori and posterior area for each of these triangles can be computed using the Shoelace Theorem Eq. (1) in its triangular form Eq. (2).

$$\mathbf{A} = \frac{1}{2}\left| \sum_{i=1}^{n-1} x_i y_{i+1} + x_n y_1 - \sum_{i=1}^{n-1} x_{i+1} y_i - x_1 y_n \right| \tag{1}$$

$$= \frac{1}{2}|x_1 y_2 + x_2 y_3 + x_3 y_1 - x_2 y_1 - x_3 y_2 - x_1 y_3 \tag{2}$$

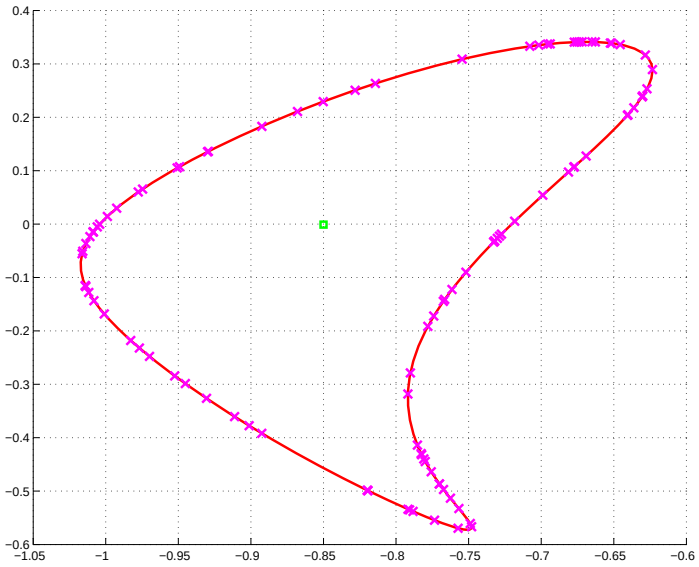

Figure 2: Comparison of Extremal Bound Algorithms in Two Dimensions

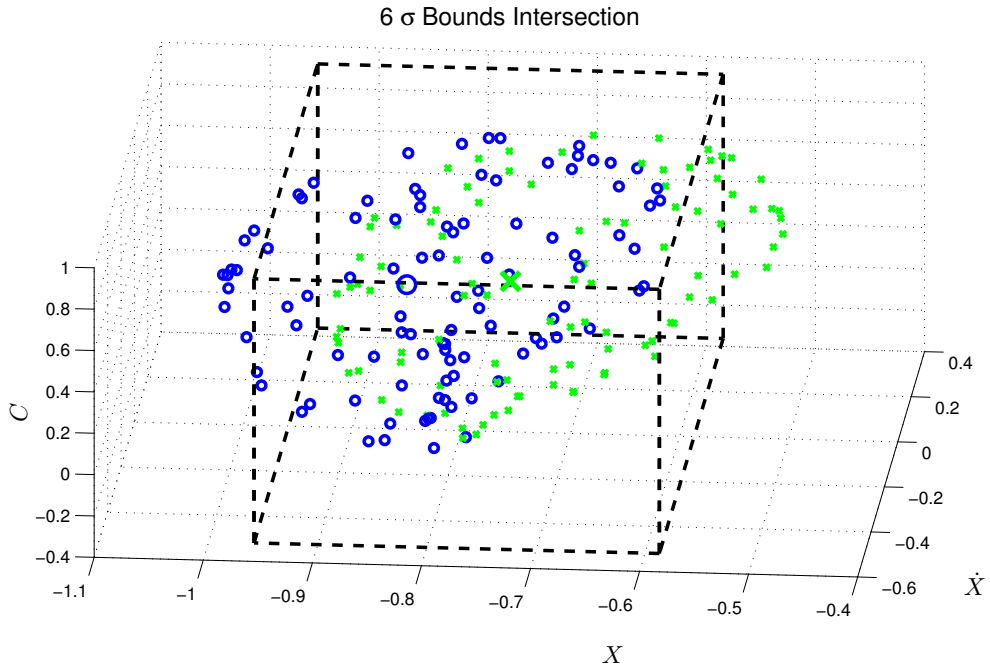

Figure 3: Intersecting Extremal Probability Region

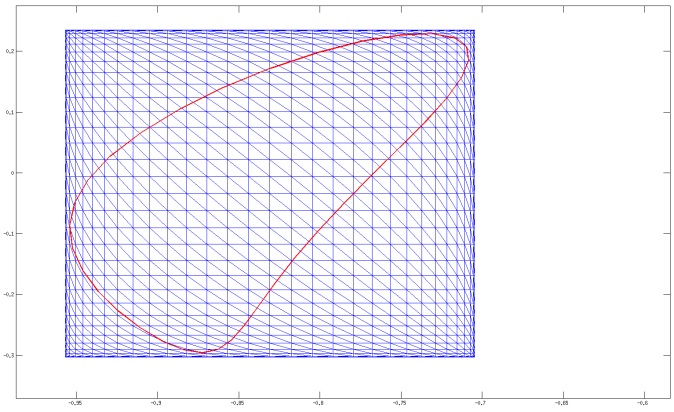

((1)) Gridded Evaluation Nodes Prior to Back-Propigation

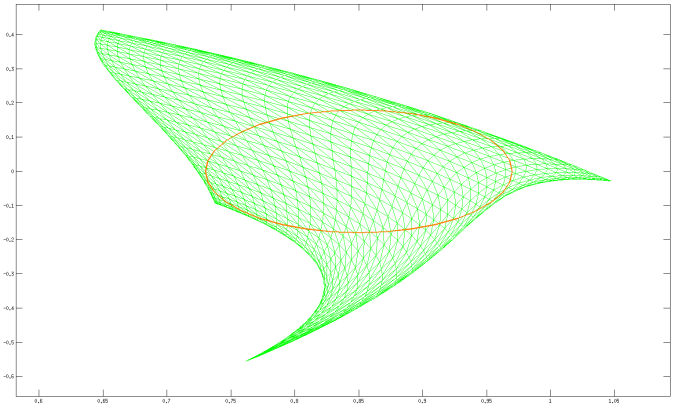

((2)) Gridded Evaluation Nodes after Back-Propigation

Figure 4: Evolution of the Area Spanned by Evaluation Nodes

A demonstration of how the area surrounding evaluation nodes can be transformed as the nodes are back-propagated to the initial time can be seen in Figure 4.

The method of accounting for volume change from 2.2 can be extended to arbitrarily high dimensions by considering the volume of an n-dimensional simplex. The equation for a generic simplex volume is shown in Eq. (3), where $v_0 ... v_n$ represent the vector locations of the simplex vertices.

$$V = \left| \frac{1}{n!} \det \left(v_1 - v_0, \quad v_2 - v_0, \quad \ldots, \quad v_n - v_0 \right) \right| \tag{3}$$

This determinate operation ($\approx O(n^3)$) clearly becomes extremely computationally intensive as n increases. It may be possible to alleviate this computational cost by using a cruder approximation to compute the volume change, but that is beyond the scope of this effort.

3. Orbital Results

OPA can be applied for various applications in the realm of space domain awareness. The most obvious application is the generation of a PDF for a planar orbit. The resulting orbit PDF is shown in Figure 5 and the cumulative probability for the PDF is demonstrated to be one over the entire PDF, as shown in Figure 6.

Table 1: Planar Orbit Parameters

	Orbit 1
a	5.466
e	0.975
M	π
t_0	0
t_f	30

Once approximation is achieved for a single RSO PDF it is possible to extend to the probability of collision for multiple RSOs, with minor modifications. This constant probability LMC is carried out for to generate the probable region in the posterior state space in all four dimensions $(X, Y, \dot{X}, \dot{Y})$, the result of which is used to define the region in X and Y that will be populated with the approximation nodes, as shown in Figure 8, [25]. The probability in the $\dot{X}$ and $\dot{Y}$ dimensions is then marginalized into the spatial dimensions for each RSO independently. The result is a pair of overlapping marginal probabilities defined at the specified approximation nodes as shown in Figure 9.

These marginal probabilities in X and Y are used to generate approximations for the probability density of the RSOs over the region of interest. The local probability of collision, $P(colision|X = x, Y = y)$ is then computed to generate an approximation for the probability of collision, as depicted in Figure 10. Finally, the total probability of collision can be computed by integrating over the resulting surface. Unfortunately, it becomes somewhat computationally impractical to extend standard OPA beyond planar orbits.

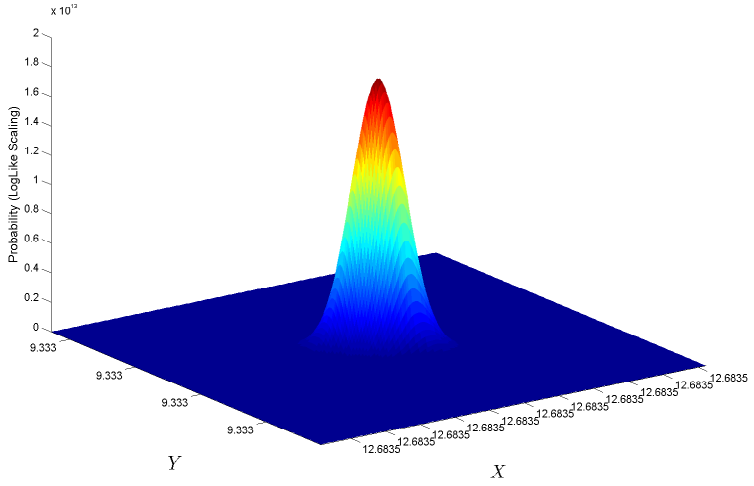

Figure 5: Spatial OPA Result for Planar Orbit

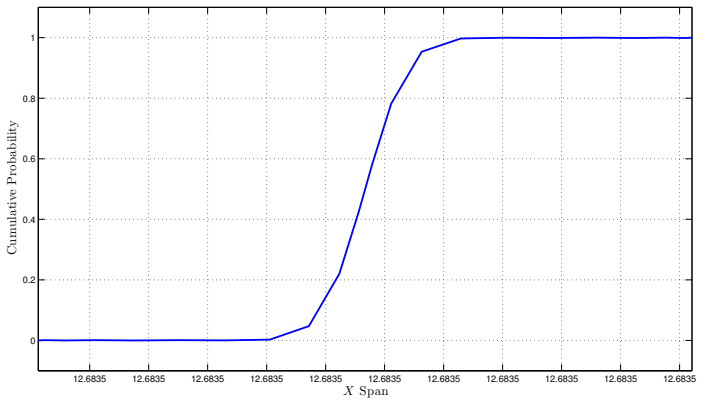

Figure 6: Cumulative Probability for Planar Orbit PDF

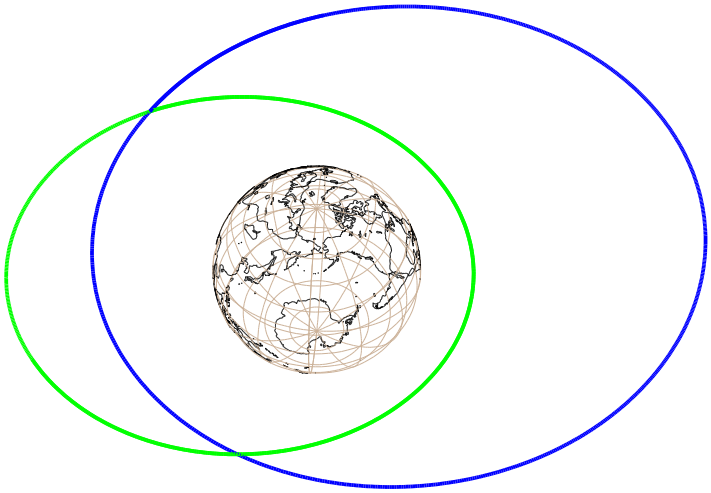

Figure 7: Planar Orbits Considered

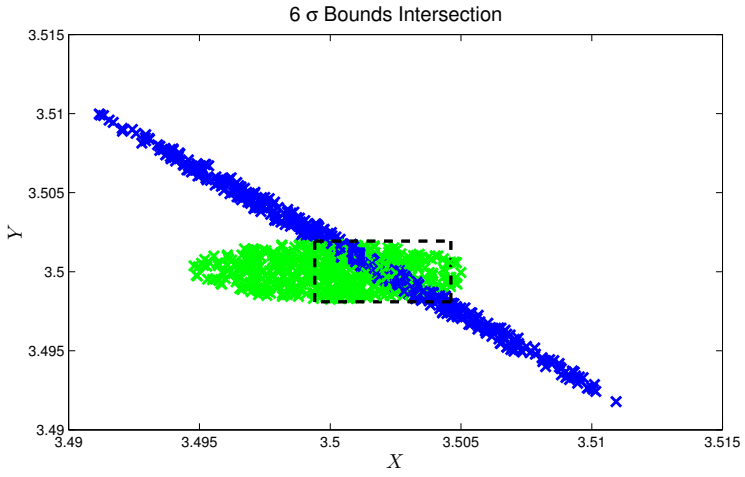

Figure 8: 6σ Orbit Intersection

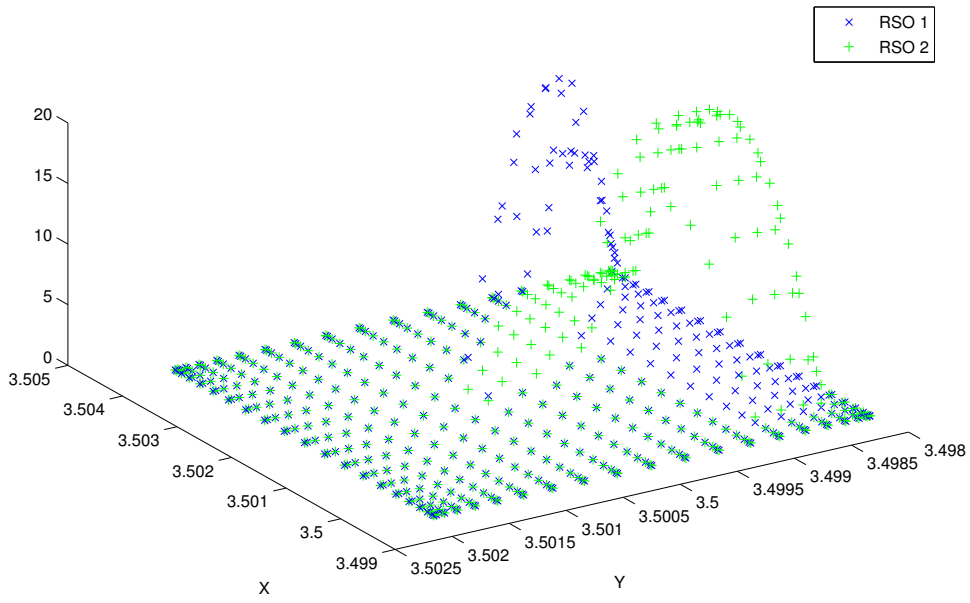

Figure 9: Overlapping RSO Marginal Probabilities

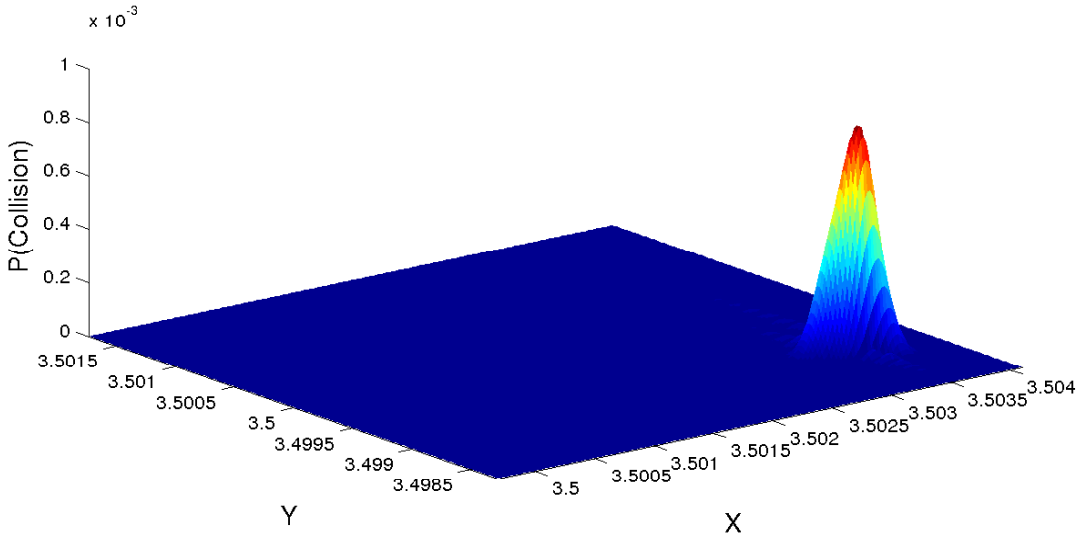

Figure 10: Probability of RSO Conjunction

3.1. Velocity Only Orbital Results

One notable application of this method that avoids the difficulties of dimensionality is predicting the position of an RSO with a known initial position but uncertainty in its initial velocity. This case is relevant for an RSO deployed from another spacecraft with an extremely well known orbital position. One example is cubesats or smallsats deployed from the International Space Station (ISS). The deployers for these small spacecraft tends to be mounted on a robotic arm and rely on a spring to push the satellite away from the ISS, resulting in approximately exact knowledge of position and uncertainty in velocity. AggieSat4, shown in Figue 11, is one example of such an RSO.

In this case the ROI is determined using the LMC holding the position fixed and varying velocity according to the probability distribution. Once the range of final positions is determined and the evaluation node grid is established the initial and final velocities that associate each node and the initial point can be determined using a Lambert solver. The initial probability can be found by comparing each initial velocity to the a-priori PDF, and the final probability can be found by modulating the initial probability based on the volumetric change. The process of applying OPA to an RSO with only initial velocity uncertainty is depicted in Figure 12, with the initial point shown as a light blue circle, the ROI in red, the evaluation nodes as dark blue x's, and a subset of Lambert trajectories in green.

A probability of collision analysis using this method was performed on two objects with the orbital properties shown in Table 2. This analysis was preformed twice with two levels of velocity uncertainty ($\sigma^2_{V_x}, \sigma^2_{V_y}, \sigma^2_{V_z}$), two different radii of collision (r_c), and various times of closest approach (T_{CA} in orbital periods) , and compared to a Monte Carlo analysis, with the results displayed in Table 3.

Table 2: Conjuncting RSO Parameters

" "	**RSO 1**	**RSO 2**
a	10000 km	10000 km
e	1.0e-7	1.0e-7
i	90.0	90.0
ω	0.0	0.0
i	0.0	90.0
σ^2_x, σ^2_y	10.0 km^2	10.0 km^2
$\sigma^2_{V_x}, \sigma^2_{V_y}$	0.01 $(km/s)^2$	0.01 $(km/s)^2$

Table 3: Probability of Collision RLMC vs MC

σ^2_V	r_c **km**	T_{CA}	PC_{LMC}	PC_{MC}	**% Error**	**MC Size (Millions)**
$1 * 10^{-7}$	0.1	0.25	1.60E-04	1.51E-04	6.4%	100
$1 * 10^{-7}$	0.1	0.75	3.68E-06	3.93E-06	6.3%	100
$1 * 10^{-7}$	0.1	1.25	4.83E-06	4.45E-06	4.5%	100
$1 * 10^{-4}$	10	0.25	5.07E-03	5.28E-03	3.9%	100
$1 * 10^{-4}$	10	0.75	1.16E-04	1.17E-04	1.0%	100
$1 * 10^{-4}$	10	1.25	1.53E-04	1.67E-04	8.6%	100

Figure 11: AggieSat4 being Deployed from the ISS

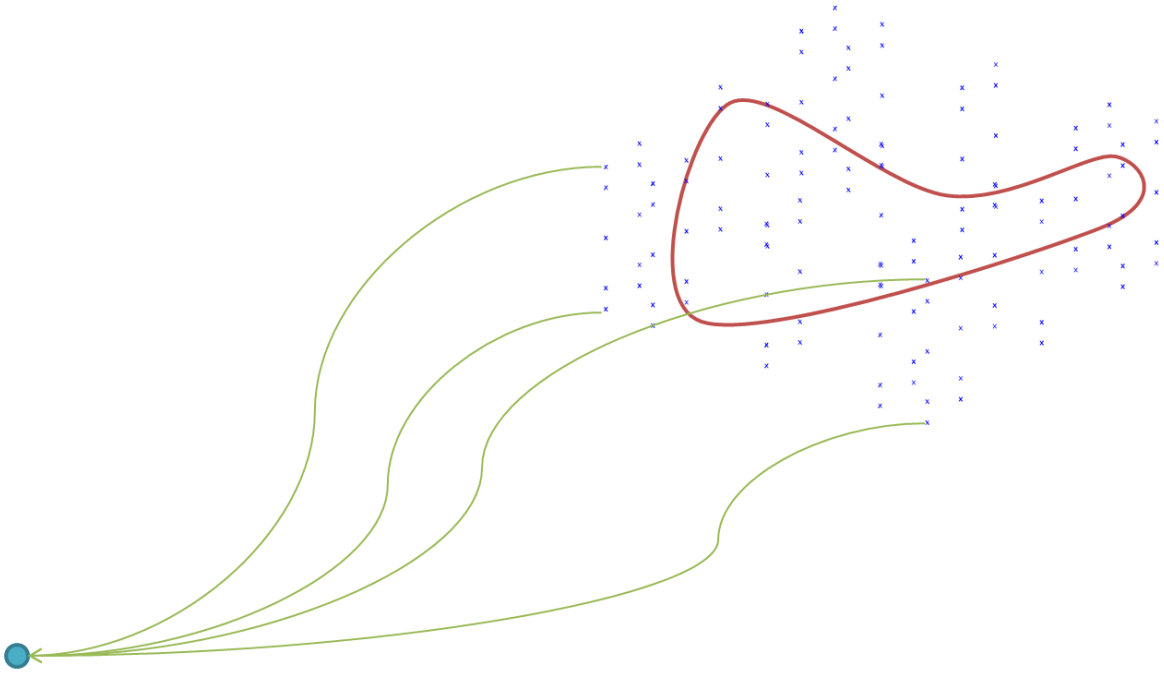

Figure 12: OPA Applied to RSO with Velocity Uncertainty

4. Further Enhancements for Orthogonal Probability Approximation for Orbital Dynamics

The main objective of this effort is to use Orthogonal Probability Approximation to perform probabilistic analysis. This requires extending OPA to work higher dimensions so that it can form approximations in a four dimensional space to examine planar orbits, the six dimensional space for a full perturbed orbital problem, and eventually even higher dimensions to examine uncertainty in the unknown parameters that govern the dynamic system. This section explains enhancements to OPA that increase its effectiveness and performance in higher dimensions.

4.1. Dimensionality

The standard version of OPA can be extended into higher dimensions with minimal modification. The obvious drawback of this is that the method clearly suffers from the curse of dimensionality. As you increase the number of dimensions the nodes required to span the space increase exponentially ($O(M^n)$ where M is the order of the approximation). This means that as the dimensionality increases standard OPA will become computationally intractable.

4.2. Region of Approximation Segmentation

One drawback of using Chebyshev polynomials as a method for approximation and integration is that they rely on cosine sampling. As a result using a standard scheme for Chebyshev polynomials results in having the lowest resolution in the center of the region of approximation and greatest resolution at the edges. This is the opposite of what is desired for the approximation of PDFs. It is preferable to have the greatest sampling near the nominal trajectory, which is generally near the center of the ROI and less information near the bounds where the probability density values are exceedingly small. This frequently results in a requirement for exceedingly high orders to achieve adequate sampling in the center of the ROI to capture the character of the PDF. Given that OPA suffers from the curse of dimensionality when considering higher dimensions this can lead to significant computational cost. A similar issue was encountered with Orbital MCPI, where achieving the required accuracy took to many evaluation nodes causing a lack of efficiency, [27]. This challenge was addressed by breaking the approximation arc into smaller segments and judiciously selecting segmentation bounds. In a similar fashion, the ROI can be broken up into smaller segments in a modified approximation and integration scheme based on repeated cosine sampling. This consists of a pair of cosine sample regions with that share an overlapping node. The overlapping node ensures the continuity of the approximate surface and allows for the use of a function evaluation in both segments. The repeated cosine sampling scheme is descried in Equations 4-6. In the case of a single PDF approximation the overlapping node, X_o is placed so that it lines up with the nominal trajectory, as shown in Figure 13, and in the case of a conjunction it is aligned with the Center of the ROI. The integral of each of the two segments is computed and the results are added together to get the full integral for the region.

$$\xi = -cos(\frac{j\pi}{M}), j = 1, 2, ..., M \tag{4}$$

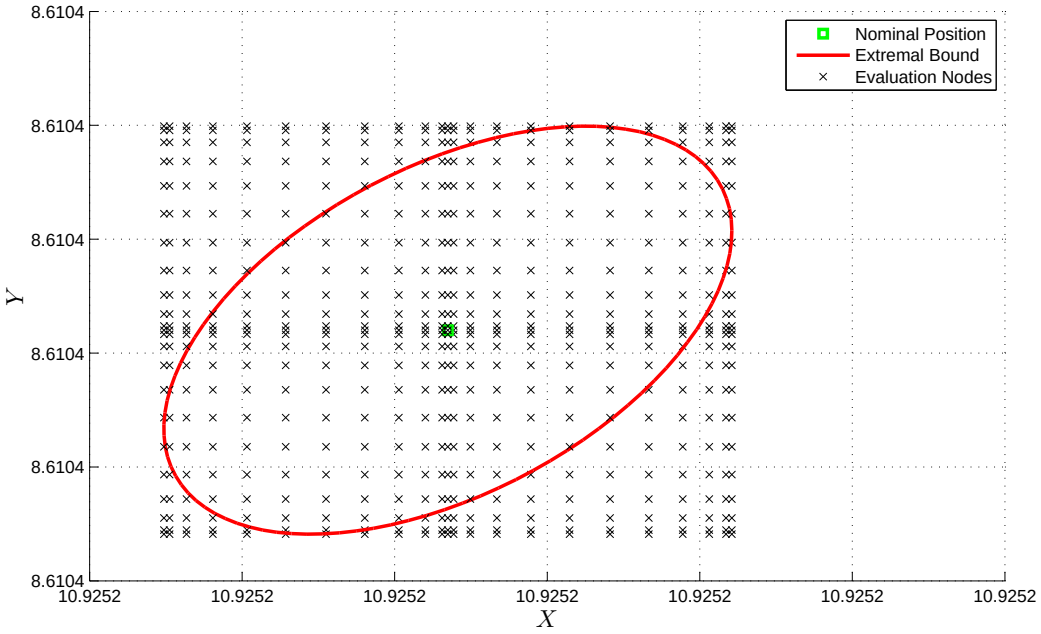

Figure 13: Segmented Repeated Cosine Sampling

$$x_{k,0,\ldots,M} = \frac{1}{2} * (\xi + 1) * (X_o - X_l) + X_l \tag{5}$$

$$x_{k,M+1,\ldots,2*M} = \frac{1}{2} * (\xi_{2,\ldots,M} + 1) * (X_u - X_o) + X_o \tag{6}$$

The considerations for volumetric change are not required when considering constant parametric dimensions of uncertainty. The distribution of nodes along these dimensions remain constant throughout the time evolution of the system, as a result of the probability density for nodes along those dimensions is also constant.

4.3. Region of Approximation Alignment

Another challenge that results from moving into higher dimensions is that the misalignment between the ROI and the distribution of the PDF results in more and more empty space as the dimension increases, resulting in greater computational cost. This cost can be reduced by transforming the ROI into a coordinate system that is better aligned with the distribution of the PDF. To achieve this the results of the LMC propagation can be used to generate a pseudo-covariance for the system, using the statistical definition for covariance. The expression for computing the pseudo-covariance for a two dimensional case is shown in Eq. (7), where $E(X_{LMC})$ and $E(Y_{LMC})$ are simply defined as the means of their respective quantities. Preforming eigen-analysis can now provide the approximate principal alignment of the PDF and provide the information required to rotate into an aligned coordinate system.

$$\text{pseudo-cov}(X, Y) = \frac{1}{n} \sum_{i=1}^{n} (x_i - E(X_{LMC}))(y_i - E(Y_{LMC})) \tag{7}$$

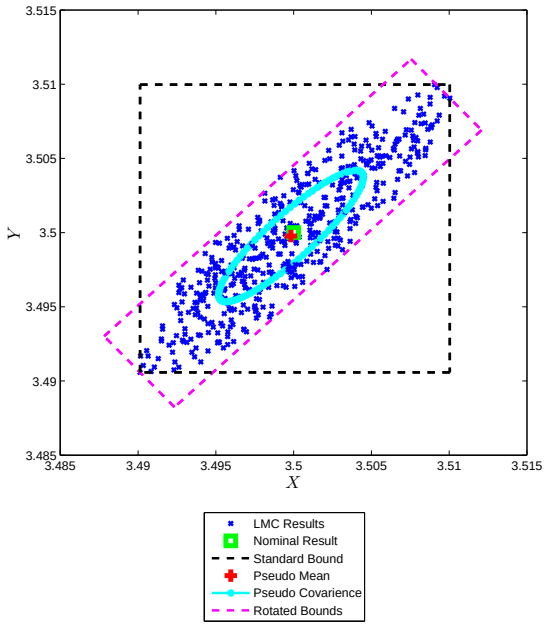

Figure 14: ROI Aligned Based on Pseudo-Covariance

A two dimensional example of this transformation is shown in Figure 14. The nominal trajectory is shown as a green square results of the initial LMC propagation are shown in blue. The mean of the LMC results is shown in red and the pseudo-covariance ellipse is plotted in cyan. The ROI was computed using the original method and again in a transformed coordinate system that is aligned with the pseudo-covariance ellipse, plotted in black and magenta, respectively. The amount of empty space from the original method is significantly greater than what results from the adjusted ROI. This reduction in empty space translates into fewer wasted function evaluation and a reduction in the required order to adequately approximate the PDF.

4.4. Marginal Dimension Isolation

For forcing functions where initial variation in the marginal dimension state components can result in wide variation of the initial state, such as the accelerations resulting from orbital dynamics, approximation of the probability integral in the marginal dimensions can be extremely difficult. This occurs because most of the marginal dimension results in no contribution to the probability, so the samples of the approximation method are wasted by incorporating a contribution of zero as opposed to sampling areas that contribute to the probability. This can be addressed by fixing the consequential dimension variables and using LMC in reverse within the marginal dimension to isolate the region that contributes to the probability. If there is a concern that the dynamics in the marginal dimension may be multi-modal a clustering algorithm, such as k-means can be used to identify the different regions of the dimension that must be considered. It is also possible to identify the portion of the marginal dimensions that contribute probability using a boundary-value solver, such as the Lambert solver from Section 3.1, a shooting method, or the Method of Particular Solutions, [28].

4.5. Dimensions of Parametric Uncertainty

It is possible to extend the method of orthogonal probability approximation to consider the effect of parametric uncertainty of a dynamic system. This is achieved by expanding the dimensions considered to include non-physical dimensions that represent possible range for the parameter of interest. Since the parameters of the dynamic system are constant through time all derivatives of any system parameter C should be 0, $\frac{\mathrm{d}C}{\mathrm{d}X} = 0$. For example if the ballistic coefficient of an orbiting spacecraft is poorly characterized, augmenting the state with a parametric dimension spanning the possible values of the ballistic coefficient allows for the system to be propagated and analyzed with OPA to evaluate with the associated probability. This dimension is then marginalized into the consequential dimensions for the final probabilistic analysis, as described in Figure 15.

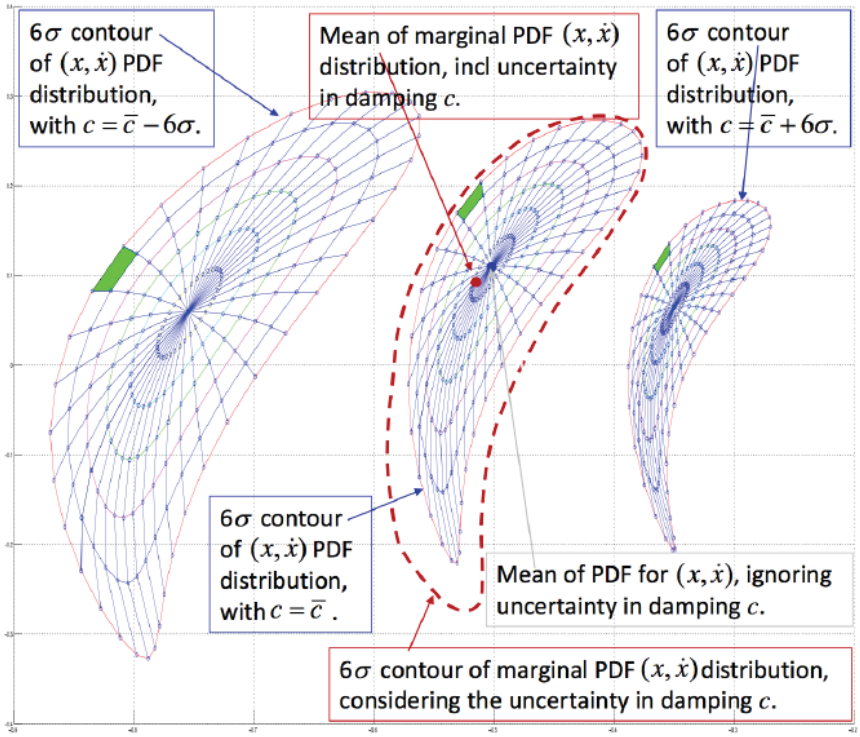

Figure 15: Damping as a Dimension of Parametric Uncertainty

5. OPA with Alternate Quadrature

One of the major drawbacks of extending OPA to higher dimensions is that it begins to suffer from the curse of dimensionality. The introduction of each new dimension results in an exponential increase in the required function evaluations. Additionally, as described in section 2.1, the cost of accounting for the volume change increases in higher dimensions. These combined factors make relying on OPA as presented in higher dimensions infeasible. Many of these difficulties result from the specifics of Clenshaw–Curtis quadrature, the method underling the approximation at the core of OPA. Clenshaw–Curtis quadrature was selected because in the consequential dimensions Multi-dimensional Clenshaw–Curtis provides the capacity for functional approximations that can then be used for the required computations. However, in the

marginal dimensions Clenshaw–Curtis was selected as a matter of convenience and compatibility with the quadrature used for the consequential dimensions. This method of quadrature can be replaced for the marginal dimensions to reduce the cost, while maintaining Clenshaw–Curtis (and the functional approximation) for the consequential dimensions. Two alternate methods of quadrature are explored, Smolyak Sparse Grid and Monte Carlo.

5.1. Sparse Grid OPA

Originally developed by Russian Mathematician Sergey Smolyak as a method for integrating and interpolating higher dimensional functions based on sparse tensor products. Instead of the representing functions with approximations based on full tensor grids Smolyak quadrature is based on a univariate quadrature rule $Q^{(1)}$. The n-dimensional Smolyak integral $Q^{(d)}$ of a function f can be written as a recursion formula with the tensor product, as shown in Eq. (8). This quadrature rule has been developed into an efficient set of weights for computational purposes, [29]. The resulting evaluation nodes for 2D and 3D can be seen in Figure 16 and Figure 17. While the number of evaluation nodes is comparable in lower dimensions (1D and 2D), Figure 18 demonstrates that as the dimension increases there are substantial cost savings.

$$Q_l^{(n)} f = \left(\sum_{i=1}^{l} \left(Q_i^{(1)} - Q_{i-1}^{(1)} \right) \otimes Q_{l-i+1}^{(n-1)} \right) f \tag{8}$$

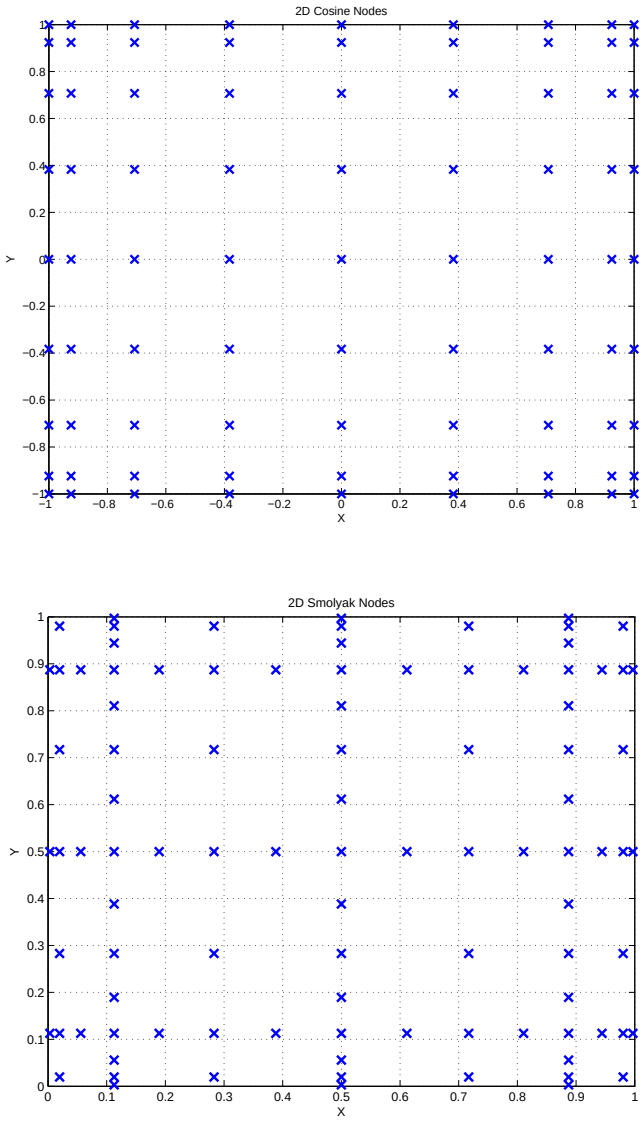

Figure 16: Comparison of Cosine and Smolyak Sampling Nodes

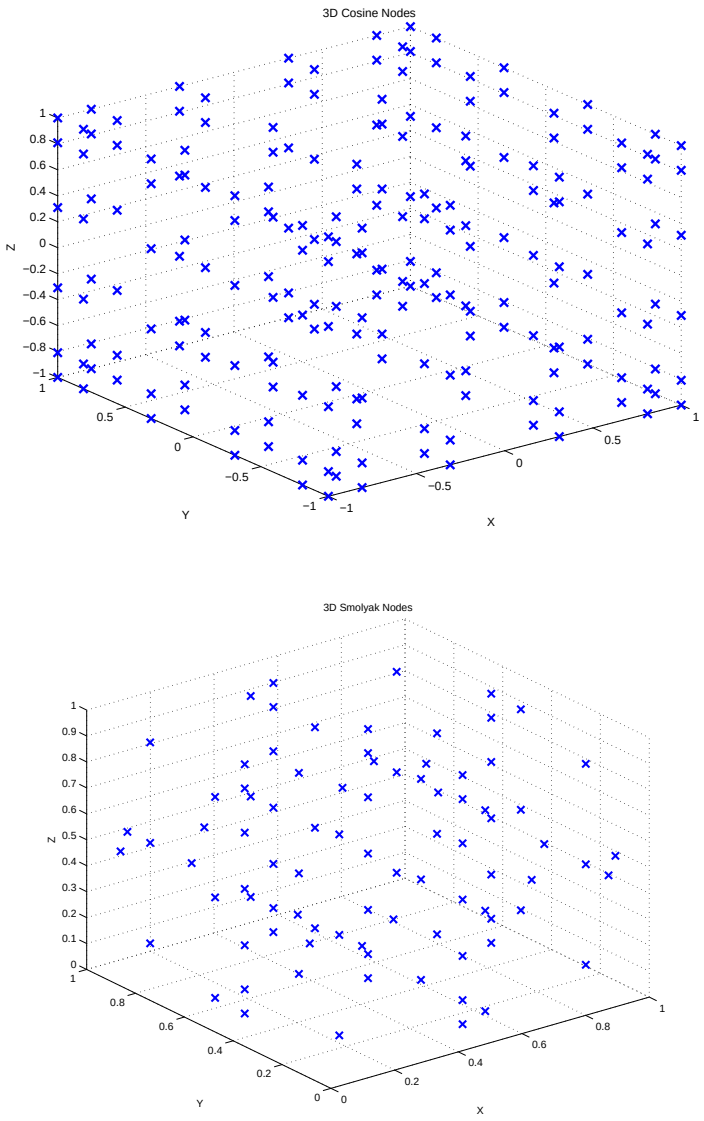

Figure 17: Comparison of Cosine and Smolyak Sampling Nodes

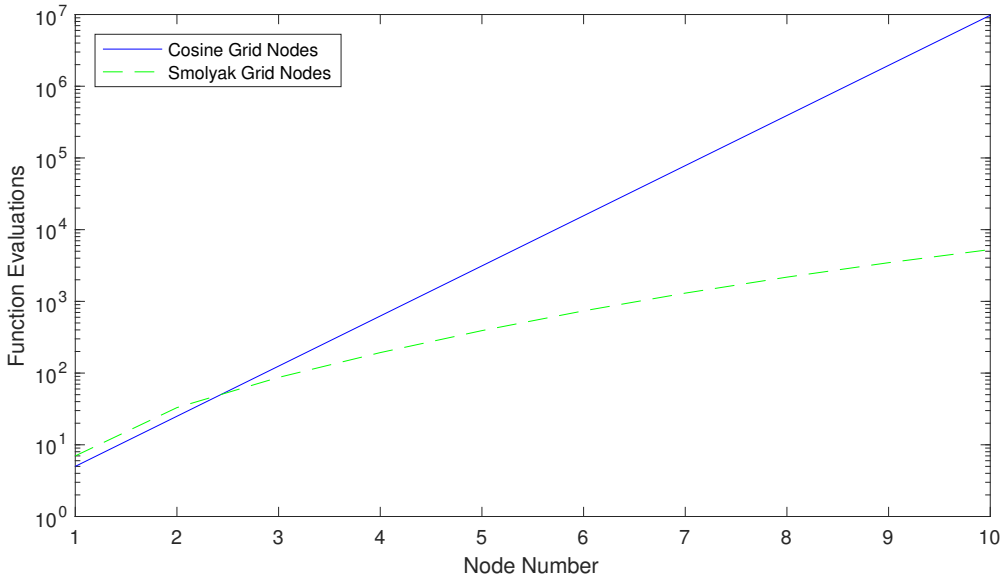

Figure 18: Comparison of Function Evaluations Required for Cosine and Smolyak Grids

This modification, Orthogonal Probability Approximation-Sparse Grid (OPA-SG), was used to propagate the uncertainty of a single RSO considering a planar orbit (four dimensions). The resulting PDF and the cumulative probability are shown in Figures 19-20. Finally, Figure 21 shows how OPA-SG being used to estimate the uncertainty of a 6-DoF orbital state. The marginal probabilities from the velocity dimensions are collapsed into the 3 spatial dimensions shown. As with previous PDF approximation examples the total probability is approximately equal to one, without being forced.

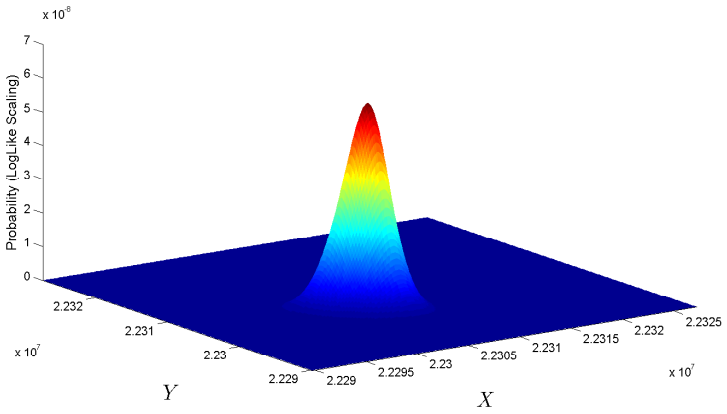

Figure 19: Approximation of PDF propagated with OPA-SG

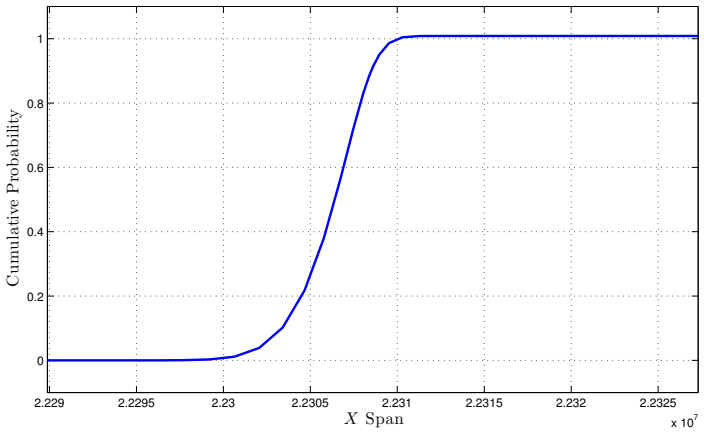

Figure 20: Cumulative Probability of PDF propagated with OPA-SG

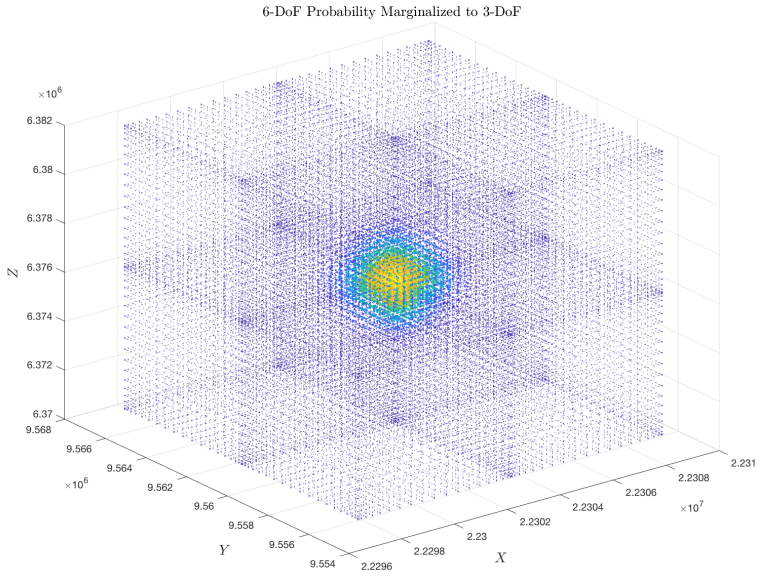

Figure 21: 6-DoF Probability Marginalized to 3-DoF

5.2. Semi-Stochastic OPA

Another method to address the failings of OPA related to the challenge of extension to higher dimensions is to modify it such that the quadrature in the marginal dimensions is preformed with with Monte Carlo (MC) or quasi-Monte Carlo (qMC) methods. Like the integration of the sparse grid quadrature techniques this leverages the advantages of OPA in the consequential dimensions while reducing the cost of high dimensional quadrature in the marginal ones. MC methods have a convergence rate of $O(N^{-}0.5)$ and qMC methods converge at a rate approaching $O(1/N)$ independent of the dimensionality, which can provide significant savings,[30]. While this method tends to be more costly than the sparse grid methods for dimensions around three, for cases with a high number of marginal dimensions it will be more efficient. Additionally, using MC or qMC methods allows for the consideration of a system that has uncertain parameters that can not be well parameterized (those driven by a random process), while standard OPA or OPA modified for use with spare grids cannot.

This modification, Orthogonal Probability Approximation-Monte Carlo (OPA-MC), was used to propagate the uncertainty of a single RSO considering a planar orbit with drag (five dimensions). The resulting PDF and the cumulative probability are shown in Figures 22 and 23.

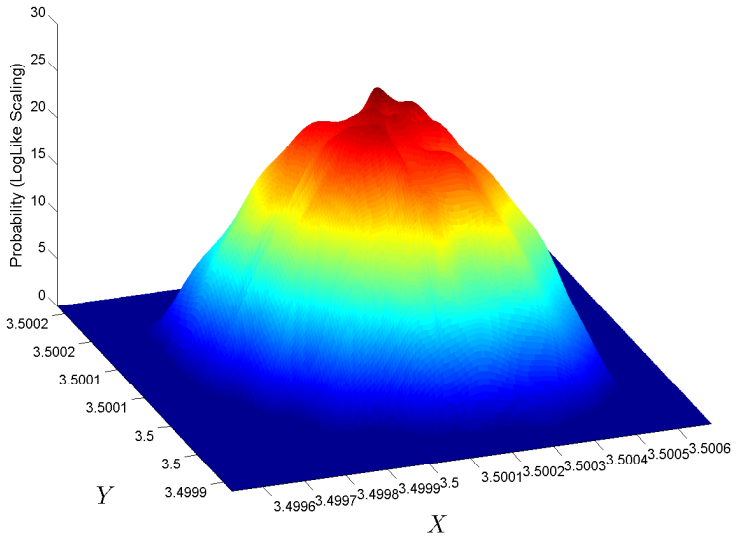

Figure 22: Approximation of PDF propagated with OPA-MC

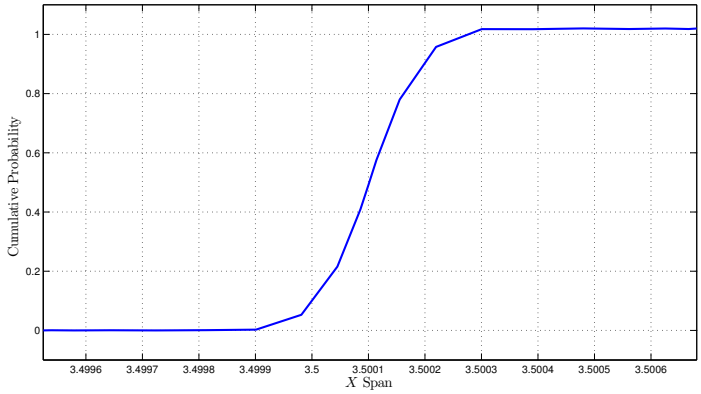

Figure 23: Cumulative Probability of PDF propagated with OPA-MC

6. Conclusion

Further development of Orthogonal Polynomial Approximation has integrated improved capabilities to approximate probability in higher dimensions. This includes the development of practical enhancements including approximation grid segmentation and region of interest alignment and the integration of parametric uncertainty. OPA was used to preform probability of collision analysis for a planar orbital collision and a 6-DoF collision in the presence of velocity uncertainty.

Additionally, two new formulations of OPA were introduced to help manage the challenges presented by the curse of dimensionality. Both of these new method use different quadrature to integrate the probability in the mrginal dimensions. The fist is OPA with sparse grid quadrature. Sparse Grid OPA relies on Smolyak quadrature to integrate the probabilities in the marginal dimensions, greatly reducing the function evaluations require especially as the dimension increases. The second new formulation, Semi-Stochastic OPA, uses stochastic methods to integrate thje marginal probabilities. This reduces the required function evaluations in higher dimensions and allows for the integration of stochastic uncertainty. These new formulations will allow OPA to be extended and used for full 6-DoF collision analysis and further to include parametric uncertainty and stochastic processes.

References

[1] D. Vallado, Fundamentals of Astrodynamics and Applications, Space Technology Library, 3rd edition, 2007.

[2] S. Alfano, Review of conjunction probability methods for short-term encounters, AAS paper (2007).

[3] S. Alfano, Satellite conjunction monte carlo analysis, AAS Spaceflight Mechanics Mtg, Pittsburgh, PA., Paper (2009) 09–233.

[4] J. R. Carpenter, Conservative analytical collision probability for design of orbital formations, 2nd International Symposium on Formation Flying (2004).

[5] J. R. Carpenter, Non-parametric collision probability for low-velocity encounters, Advances in Astronautical Sciences: AAS/AIAA Space Flight Mechanics Meeting (2007).

[6] J. R. Carpenter, F. L. Markley, D. Gold, Sequential probability ratio test for collision avoidance maneuver decisions, The Journal of the Astronautical Sciences 59 (2012) 267–280.

[7] S. R. Chesley, P. W. Chodas, Asteroid close approaches: analysis and potential impact detection, Asteroids III (2002) 55.

[8] D.-H. Cho, Y. Chung, H. Bang, Trajectory correction maneuver design using an improved b-plane targeting method, Acta Astronautica 72 (2012) 47–61.

[9] J. Foster, H. S. Estes, A parametric analysis of orbital debris collision probability and maneuver rate for space vehicles, NASA JSC 25898 (1992).
[10] M. R. Akella, K. T. Alfriend, Probability of collision between space objects, Journal of Guidance, Control, and Dynamics 23 (2000) 769–772.
[11] F. K. Chan, Spacecraft collision probability, Aerospace Press El Segundo, CA, 2008.
[12] A. Fuller, Analysis of nonlinear stochastic systems by means of the fokker–planck equation, International Journal of Control 9 (1969) 603–655.
[13] M. Kumar, S. Chakravorty, P. Singla, J. L. Junkins, The partition of unity finite element approach with hp-refinement for the stationary fokker–planck equation, Journal of Sound and Vibration 327 (2009) 144–162.
[14] Y. Sun, M. Kumar, Numerical solution of high dimensional stationary fokker–planck equations via tensor decomposition and chebyshev spectral differentiation, Computers & Mathematics with Applications 67 (2014) 1960–1977.
[15] K. Vishwajeet, P. Singla, M. Jah, Nonlinear uncertainty propagation for perturbed two-body orbits, Journal of Guidance, Control, and Dynamics 37 (2014) 1415–1425.
[16] C. Sabol, C. Binz, A. Segerman, K. Roe, P. W. Schumacher Jr, Probability of collision with special perturbations dynamics using the monte carlo method, in: AAS/AIAA Astrodynamics Specialist Conference, Girdwood, AK.
[17] G. Terejanu, P. Singla, T. Singh, P. D. Scott, Uncertainty propagation for nonlinear dynamic systems using gaussian mixture models, Journal of Guidance, Control, and Dynamics 31 (2008) 1623–1633.
[18] P. De Valpine, Monte carlo state-space likelihoods by weighted posterior kernel density estimation, Journal of the American Statistical Association 99 (2004) 523–536.
[19] J. T. Horwood, N. D. Aragon, A. B. Poore, Gaussian sum filters for space surveillance: theory and simulations, Journal of Guidance, Control, and Dynamics 34 (2011) 1839–1851.
[20] K. J. DeMars, R. H. Bishop, M. K. Jah, Entropy-based approach for uncertainty propagation of nonlinear dynamical systems, Journal of Guidance, Control, and Dynamics 36 (2013) 1047–1057.
[21] C. Roscoe, I. Hussein, M. Wilkins, P. Schumacher, The probabilistic admissible region with additional constraints, in: Proceedings of the Advanced Maui Optical and Space Surveillance Technologies Conference, held in Wailea, Maui, Hawaii, September 15-18, 2014, Ed.: S. Ryan, The Maui Economic Development Board, id. 91, volume 1, p. 91.
[22] R. Ghanem, P. Spanos, Polynomial chaos in stochastic finite elements, Journal of Applied Mechanics 57 (1990) 197–202.
[23] M. Eldred, J. Burkardt, Comparison of non-intrusive polynomial chaos and stochastic collocation methods for uncertainty quantification, AIAA paper 976 (2009) 1–20.
[24] B. A. Jones, A. Doostan, G. H. Born, Nonlinear propagation of orbit uncertainty using non-intrusive polynomial chaos, Journal of Guidance, Control, and Dynamics 36 (2013) 430–444.
[25] A. Probe, T. A. Elgohary, J. L. Junkins, A new method for space objects probability of collision, in: AIAA/AAS Astrodynamics Specialist Conference, p. 5653.
[26] S. Smale, Mathematical problems for the next century, Mathematical Intelligencer 20 (1998) 7–15.
[27] B. Macomber, R. Probe, A. Woollands, J. Read, , J. Junkins, Enhancements for modified chebyshev-picard iteration efficiency for perturbed orbit propagation, Computer Modeling in Engineering Sciences (Sumbitted 2015).
[28] R. M. Woollands, J. L. Read, A. B. Probe, J. L. Junkins, Multiple revolution solutions for the perturbed lambert problem using the method of particular solutions and picard iteration, The Journal of the Astronautical Sciences 64 (2017) 361–378.
[29] F. Heiss, V. Winschel, Likelihood approximation by numerical integration on sparse grids, Journal of Econometrics 144 (2008) 62–80.
[30] S. Asmussen, P. W. Glynn, Stochastic simulation: algorithms and analysis, volume 57, Springer Science & Business Media, 2007.